

Structural Health Monitoring and Resonance Frequency Analysis of Internal Damage In Isotropic Laminated Plates

Mao-Hsuan Chang, Shih-Hao Lin and Ching-Yuan Chang*

Abstract—Composite plates are a structural solution that enhances material stiffness and reduces structural weight. For instance, the introduction of glass fiber-reinforced materials in wind turbine blades improves tensile strength in specific directions, thereby reducing system weight and increasing power generation efficiency. Additionally, composite plates enhance structural rigidity due to the directional nature of the interlayer fibers. However, the anisotropic nature of composite materials can lead to internal damage when external stresses are not aligned with the fiber distribution. In practical systems, forces act in various directions, posing fatigue and damage risks to the inner layers of composite plates. The objective of this study is to initially assume isotropic properties for all plates to simplify the complexity of theoretical validation. By applying Kirchhoff's plate theory, internal force equilibrium equations are established for intact and damaged plates. Subsequently, the force equilibrium equations for all plates are summed to derive the governing equation for out-of-plane displacements of isotropic plates. Neglecting material damping coefficients, the out-of-plane motion of plates is assumed to follow harmonic motion, and the resonant frequency of the structure is calculated and compared with that of a damaged structure. Through this research, a better understanding of the impact of structural integrity and internal damage on resonant frequency response can be achieved. Further investigations will focus on exploring the effects of different stacking sequences and proposing methods to calculate the influence of resonance frequencies for various plate configurations. This will contribute to improving the design and analysis of laminated structures, providing more accurate and reliable guidance to ensure structural safety and performance.

I. INTRODUCTION

In the design of aircraft wings or fan blades, it is crucial to avoid the natural frequencies of the structure coinciding with the operating frequencies. When the natural frequency of a structure matches the operating frequency, resonance phenomena can occur, leading to structural damage or failure, posing significant safety risks. However, regardless of how carefully designed, accurately predicting the damage caused by fatigue or external force impact during the initial design phase is challenging. This is because fatigue damage is a progressive process, while external force impacts can be sudden events that are difficult to predict accurately. Therefore, laminated plate damage analysis becomes a critical approach. Engineers employ the finite element method to simulate laminated plates and evaluate the structural strength and damage states. The finite element method can provide stress distribution, regions of strain concentration, and potential crack locations, assisting engineers in understanding

the durability and reliability of the structure. However, the finite element method also has its limitations. Firstly, establishing an accurate finite element model requires complex geometric modeling and mesh generation of the structure, which can consume significant time and human resources. Secondly, the accuracy of the finite element method is influenced by model assumptions and input parameters, introducing uncertainties in the model. Additionally, the finite element method presents challenges when simulating complex damage patterns and crack propagation. In conclusion, laminated plate damage analysis is a crucial process in the design and evaluation of aircraft wings or fan blade structures. While the finite element method is a widely used analytical tool, engineers should be aware of its limitations and complement it with other inspection techniques and experimental validations to comprehensively assess the safety and reliability of the structure.

II. THEORETICAL MODEL CONSTRUCTION

In this section, we will introduce the Kirchhoff plate theory model and its application to isotropic laminated plates. The utilization of the Kirchhoff plate theory is justified due to its close approximation to the stress conditions experienced by structures such as wind turbine blades and wings. The predominant loading state in wings and blades involves external forces perpendicular to the surface of the structure. The assumptions of the Kirchhoff plate theory state that the stresses in the z-direction (thickness direction) are negligible compared to those in the x and y directions (in-plane directions), and that there are no transverse shear stresses on the plate surface. Therefore, complex three-dimensional problems can be simplified into two-dimensional problems.

A. Kirchhoff Plate Theory

In this study, the Kirchhoff plate theory is employed to describe the out-of-plane displacement equations for each layer of the laminate. The displacement fields in the x-direction, denoted as u , in the y-direction as v , and in the z-direction as w , are considered. The Kirchhoff plate theory assumes that the stresses in the z-direction are negligibly small compared to those in the x and y directions. This assumption allows for the simplification of the three-dimensional problem into a two-dimensional problem. The displacement fields are defined as shown in equation (1).

$$\begin{aligned}
u &= -z \frac{\partial w}{\partial x} \\
v &= -z \frac{\partial w}{\partial y} \\
w &= w(x, y)
\end{aligned} \quad (1)$$

The relationship between strain and displacement fields is described by equation (2).

$$\begin{aligned}
\varepsilon_{xx} &= \frac{\partial u}{\partial x} = -z \frac{\partial^2 w}{\partial x^2} \\
\varepsilon_{yy} &= \frac{\partial v}{\partial y} = -z \frac{\partial^2 w}{\partial y^2} \\
\gamma_{xy} &= 2 \left(\frac{\partial u}{\partial y} + \frac{\partial v}{\partial x} \right) = -2z \frac{\partial^2 w}{\partial y^2}
\end{aligned} \quad (2)$$

In Kirchhoff's plate theory, the surface strain is the sum of the mid-plane strain and the product of the mid-plane to surface thickness and the tangent gradient. This allows us to express the strain in terms of the displacement field as shown in equation (3).

$$\begin{aligned}
\varepsilon_{xx} &= \frac{\partial u_0}{\partial x} - z \frac{\partial^2 w}{\partial x^2} \\
\varepsilon_{yy} &= \frac{\partial v_0}{\partial y} - z \frac{\partial^2 w}{\partial y^2} \\
\gamma_{xy} &= \frac{\partial u_0}{\partial y} + \frac{\partial v_0}{\partial x} - 2z \frac{\partial^2 w}{\partial y^2}
\end{aligned} \quad (3)$$

The conversion between two-dimensional strain and stress needs to consider the Poisson's ratio, which can be expressed by equation (4).

$$\begin{aligned}
\sigma_{xx} &= \frac{E}{1-\nu^2} (\varepsilon_{xx} + \nu \varepsilon_{yy}) \\
\sigma_{yy} &= \frac{E}{1-\nu^2} (\varepsilon_{yy} + \nu \varepsilon_{xx}) \\
\tau_{xy} &= \frac{E}{2(1+\nu)} \gamma_{xy}
\end{aligned} \quad (4)$$

By integrating the stress along the thickness direction, the stress field can be obtained. By multiplying the stress by the thickness and integrating it along the thickness direction, the bending moment field can be obtained. The stress field, denoted as N_{ij} , is given by equation (5), and the bending moment field, denoted as M_{ij} , is given by equation (6).

$$\begin{bmatrix} N_{xx} \\ N_{yy} \\ N_{xy} \end{bmatrix} = \int_{-\frac{h}{2}}^{\frac{h}{2}} \begin{bmatrix} \sigma_{xx} \\ \sigma_{yy} \\ \sigma_{xy} \end{bmatrix} dz \quad (5)$$

$$\begin{bmatrix} M_{xx} \\ M_{yy} \\ M_{xy} \end{bmatrix} = \int_{-\frac{h}{2}}^{\frac{h}{2}} \begin{bmatrix} \sigma_{xx} \\ \sigma_{yy} \\ \sigma_{xy} \end{bmatrix} z dz \quad (6)$$

Although the Kirchhoff thin plate theory assumes that the stress in the z-axis direction is much smaller than the stresses in the other axial directions, the transverse shear stress cannot be neglected in the equilibrium equations. The transverse shear stress field is defined by equation (7).

$$\begin{bmatrix} Q_x \\ Q_y \end{bmatrix} = \int_{-\frac{h}{2}}^{\frac{h}{2}} \begin{bmatrix} \sigma_{xz} \\ \sigma_{yz} \end{bmatrix} dz \quad (7)$$

The equilibrium equations for the bending moment field and the transverse shear force are given by equation (8).

$$\begin{aligned}
\frac{\partial M_{xx}}{\partial x} + \frac{\partial M_{xy}}{\partial y} &= Q_x \\
\frac{\partial M_{yy}}{\partial y} + \frac{\partial M_{xy}}{\partial x} &= Q_y
\end{aligned} \quad (8)$$

If external forces are present on the thin plate, the sum of the partial derivatives of the transverse shear force with respect to x and y will be equal to the external force. This relationship can be used as an equilibrium equation with external forces, as shown in equation (9).

$$\frac{\partial Q_x}{\partial x} + \frac{\partial Q_y}{\partial y} = -q \quad (9)$$

By considering the kinetic energy resulting from the mass of the thin plate, the equilibrium equation mentioned above can be rearranged to obtain the governing equation for the out-of-plane displacement of the thin plate. This equation is represented by equation (10).

$$D \left(\frac{\partial^4 w}{\partial x^4} + 2 \frac{\partial^4 w}{\partial x^2 \partial y^2} + \frac{\partial^4 w}{\partial y^4} \right) + \rho h \frac{\partial^2 w}{\partial t^2} = 0 \quad (10)$$

B. Classical Laminate Plate Theory

The governing equation for the displacement of a laminated composite plate is constructed based on the Kirchhoff plate theory. Unlike a single-layer plate, the orientation of the laminated materials in the composite plate affects the calculation results. In this section, we will introduce the strain transformation relationships for materials with different orientations. By summing up the stress field and bending moment field of each thin layer, the stress field and bending moment field of the laminated composite plate are obtained. Here, 'k' represents the number of layers. The relationships are shown in equations (11) and (12).

$$\begin{bmatrix} N_{xx} \\ N_{yy} \\ N_{xy} \end{bmatrix} = \sum_{k=1}^n \int_{z_{k-1}}^{z_k} \begin{bmatrix} \sigma_{xx} \\ \sigma_{yy} \\ \sigma_{xy} \end{bmatrix} dz \quad (11)$$

$$\begin{bmatrix} M_{xx} \\ M_{yy} \\ M_{xy} \end{bmatrix} = \sum_{k=1}^n \int_{z_{k-1}}^{z_k} \begin{bmatrix} \sigma_{xx} \\ \sigma_{yy} \\ \sigma_{xy} \end{bmatrix} z dz \quad (12)$$

The material coefficients and stress-strain relationships for each layer are given by equations (13) and (14).

$$\begin{bmatrix} \varepsilon_{xx} \\ \varepsilon_{yy} \\ \frac{\gamma_{xy}}{2} \end{bmatrix} = \begin{bmatrix} \frac{1}{E_{xx}} & -\frac{\nu}{E_{xx}} & 0 \\ -\frac{\nu}{E_{xx}} & \frac{1}{E_{yy}} & 0 \\ 0 & 0 & \frac{1}{G_{xy}} \end{bmatrix} \begin{bmatrix} \sigma_{xx} \\ \sigma_{yy} \\ \sigma_{xy} \end{bmatrix} \quad (13)$$

$$\begin{bmatrix} \sigma_{xx} \\ \sigma_{yy} \\ \tau_{xy} \end{bmatrix} = \begin{bmatrix} Q_{11} & Q_{12} & Q_{16} \\ Q_{21} & Q_{22} & Q_{26} \\ Q_{61} & Q_{62} & 2Q_{66} \end{bmatrix} \begin{bmatrix} \varepsilon_{xx} \\ \varepsilon_{yy} \\ \frac{\gamma_{xy}}{2} \end{bmatrix} \quad (14)$$

The Q matrix, which is the inverse of the material coefficient matrix, is given by equation (15).

$$[Q] = [S]^{-1} \quad (15)$$

The stress transformation relationship for anisotropic materials is expressed by equation (16).

$$\begin{bmatrix} \sigma_{11} \\ \sigma_{22} \\ \tau_{12} \end{bmatrix} = \begin{bmatrix} \cos^2 \alpha & \sin^2 \alpha & 2\cos \alpha \sin \alpha \\ \sin^2 \alpha & \cos^2 \alpha & -2\cos \alpha \sin \alpha \\ -\cos \alpha \sin \alpha & \cos \alpha \sin \alpha & \cos^2 \alpha - \sin^2 \alpha \end{bmatrix} \begin{bmatrix} \sigma_{xx} \\ \sigma_{yy} \\ \tau_{xy} \end{bmatrix} \quad (16)$$

Substituting the stress transformation relationship given by equation (17) into the strain, the strain transformation relationship is obtained as shown in equation (18).

$$[T] = \begin{bmatrix} \cos^2 \alpha & \sin^2 \alpha & 2\cos \alpha \sin \alpha \\ \sin^2 \alpha & \cos^2 \alpha & -2\cos \alpha \sin \alpha \\ -\cos \alpha \sin \alpha & \cos \alpha \sin \alpha & \cos^2 \alpha - \sin^2 \alpha \end{bmatrix} \quad (17)$$

$$\begin{bmatrix} \sigma_{xx} \\ \sigma_{yy} \\ \tau_{xy} \end{bmatrix} = [T]^{-1} [Q] [T] \begin{bmatrix} \varepsilon_{xx} \\ \varepsilon_{yy} \\ \varepsilon_{xy} \end{bmatrix} = [\bar{Q}] \begin{bmatrix} \varepsilon_{xx} \\ \varepsilon_{yy} \\ \varepsilon_{xy} \end{bmatrix} \quad (18)$$

The Q matrix is a constant matrix constructed from the material coefficients and the material orientation angles. Its relationship is given by equations (19) and (20).

$$\begin{aligned} \bar{Q}_{11} &= U_1 + U_2 \cos 2\theta + U_3 \cos 4\theta \\ \bar{Q}_{12} &= U_4 - U_3 \cos 4\theta \\ \bar{Q}_{22} &= U_1 - U_2 \cos 2\theta + U_3 \cos 4\theta \\ \bar{Q}_{66} &= U_5 - U_3 \cos 4\theta \\ \bar{Q}_{16} &= \frac{1}{2} U_2 \sin 2\theta + U_3 \sin 4\theta \\ \bar{Q}_{26} &= \frac{1}{2} U_2 \sin 2\theta - U_3 \sin 4\theta \\ U_1 &= \frac{1}{8} (3Q_{11} + 3Q_{22} + 2Q_{12} + 4Q_{66}) \\ U_2 &= \frac{1}{2} (Q_{11} - Q_{22}) \\ U_3 &= \frac{1}{8} (Q_{11} + Q_{22} - 2Q_{12} - 4Q_{66}) \\ U_4 &= \frac{1}{8} (Q_{11} + Q_{22} + 6Q_{12} - 4Q_{66}) \\ U_5 &= \frac{1}{2} (U_1 - U_4) \end{aligned} \quad (19)$$

By substituting all the aforementioned equations into the thin plate strain field equation, which includes the mid-plane strain and the product of mid-plane to surface thickness and the tangent slope (referred to as curvature strain), we obtain equations (21) and (22).

$$\begin{bmatrix} N_{xx} \\ N_{yy} \\ N_{xy} \end{bmatrix} = \int_{-\frac{h}{2}}^{\frac{h}{2}} [\bar{Q}] \left(\begin{bmatrix} \varepsilon_{xx}^0 \\ \varepsilon_{yy}^0 \\ \varepsilon_{xy}^0 \end{bmatrix} + z \begin{bmatrix} \kappa_{xx} \\ \kappa_{yy} \\ \kappa_{xy} \end{bmatrix} \right) dz \quad (21)$$

$$\begin{bmatrix} M_{xx} \\ M_{yy} \\ M_{xy} \end{bmatrix} = \int_{-\frac{h}{2}}^{\frac{h}{2}} [\bar{Q}] \left(\begin{bmatrix} \varepsilon_{xx}^0 \\ \varepsilon_{yy}^0 \\ \varepsilon_{xy}^0 \end{bmatrix} + z \begin{bmatrix} \kappa_{xx} \\ \kappa_{yy} \\ \kappa_{xy} \end{bmatrix} \right) z dz \quad (22)$$

Since the Q matrix is constant, the integral terms of the stress field and the bending moment field can be grouped into constant matrices A, B, and D, as shown in equations (23) and (24).

$$\begin{bmatrix} N_{xx} \\ N_{yy} \\ N_{xy} \end{bmatrix} = [A_{ij}] \begin{bmatrix} \varepsilon_{0xx} \\ \varepsilon_{0yy} \\ \varepsilon_{0xy} \end{bmatrix} + [B_{ij}] \begin{bmatrix} \kappa_{xx} \\ \kappa_{yy} \\ \kappa_{xy} \end{bmatrix} \quad (23)$$

$$\begin{bmatrix} M_{xx} \\ M_{yy} \\ M_{xy} \end{bmatrix} = [B_{ij}] \begin{bmatrix} \varepsilon_{0xx} \\ \varepsilon_{0yy} \\ \varepsilon_{0xy} \end{bmatrix} + [D_{ij}] \begin{bmatrix} \kappa_{xx} \\ \kappa_{yy} \\ \kappa_{xy} \end{bmatrix} \quad (24)$$

The matrix A represents the tensile stiffness, the matrix B represents the coupling between bending and tension, and the matrix D represents the bending stiffness. Expanding these matrices yields equation (25).

$$\begin{aligned}
A_{ij} &= \sum_{k=1}^n \bar{Q}^k (z_k - z_{k-1}) \\
B_{ij} &= \frac{1}{2} \sum_{k=1}^n \bar{Q}^k (z_k^2 - z_{k-1}^2) \\
D_{ij} &= \frac{1}{3} \sum_{k=1}^n \bar{Q}^k (z_k^3 - z_{k-1}^3)
\end{aligned} \quad (25)$$

This study aims to investigate the variations in the resonance frequencies of internal damage in symmetric laminated plates composed of identical isotropic materials. Therefore, the coupling stiffness matrix, which represents the bending-stretching coupling effect, can be neglected. By rearranging the equilibrium equations based on Kirchhoff's plate theory, a governing equation similar to that of a single-layer plate can be derived. Equation (26) represents this governing equation, with the main difference lying in the integration thickness for the bending moment field and stress field.

$$D \left(\frac{\partial^4 w}{\partial x^4} + 2 \frac{\partial^4 w}{\partial x^2 \partial y^2} + \frac{\partial^4 w}{\partial y^4} \right) + \rho h \frac{\partial^2 w}{\partial t^2} = 0 \quad (26)$$

C. Resonance frequencies of a damaged single-layer plate.

To simplify the problem, two assumptions are made in the preliminary construction of the displacement equation for the damaged thin plate. First, the damaged region of the plate is assumed to have a closed and simple geometric shape, which is defined in this study as a rectangle. Second, there are no residual stresses at the boundary between the damaged and undamaged regions.

The assumption of no residual stresses is made because residual stresses can alter the local material properties and their distribution is nonlinear, which would complicate the analysis. Therefore, this factor is not considered at this stage. Since the damaged thin plate is discontinuous in its coordinates, it is not possible to construct a global equation of motion using thin plate theory. In this study, the differential energy method is employed, treating the damaged and undamaged regions as separate and independent systems. The kinetic and strain energies of these two independent systems are obtained using the Lagrangian equations of motion, and their relationship is given by Equation (27).

$$\begin{aligned}
U_{total} &= U_{no-damage} - U_{damage} \\
T_{total} &= T_{no-damage} - T_{damage}
\end{aligned} \quad (27)$$

Please note that Equation (27) represents the relationship between kinetic and strain energies derived from the differential energy method, considering the assumptions of a closed and simple geometric shape for the damaged region and the absence of residual stresses at the boundary.

By subtracting the difference in kinetic energies and potential energies of the two systems, the minimum potential energy of the overall system is obtained. This means that the total kinetic

energy is equal to the total strain energy, as shown in Equation (28).

$$L = U_{total} - T_{total} \quad (28)$$

Please note that Equation (28) represents the equality between the total kinetic energy and total strain energy, derived from the differential energy method and the assumption of no residual stresses.

By doing so, the issue of geometric discontinuity can be resolved. The total potential energy function can then be used in conjunction with the analytical thin plate motion equation to obtain the governing equations of motion for the damaged plate.

Please note that the use of the analytical thin plate motion equation allows for the determination of the motion equation for the damaged plate based on the obtained total potential energy function.

D. Resonance frequencies of damaged laminated composite plates.

By substituting the differential equations obtained from equation (28) into equations (5) and (6), the governing equations of motion for the damaged plate can be derived, as shown in equations (29) and (30).

$$\begin{bmatrix} N_{xx,damage} \\ N_{yy,damage} \\ N_{xy,damage} \end{bmatrix} = \int_{-\frac{h}{2}}^{\frac{h}{2}} \begin{bmatrix} \sigma_{xx,damage} \\ \sigma_{yy,damage} \\ \sigma_{xy,damage} \end{bmatrix} dz \quad (29)$$

$$\begin{bmatrix} M_{xx,damage} \\ M_{yy,damage} \\ M_{xy,damage} \end{bmatrix} = \int_{-\frac{h}{2}}^{\frac{h}{2}} \begin{bmatrix} \sigma_{xx,damage} \\ \sigma_{yy,damage} \\ \sigma_{xy,damage} \end{bmatrix} z dz \quad (30)$$

Equations (29) and (30) represent the shear stress field and bending moment field of the damaged plate, while equations (5) and (6) represent the undamaged plates in the upper and lower layers. By substituting equations (5), (6), (29), and (30) into equations (23) and (24), the stiffness matrices and bending moment matrices of the laminated plate with internal damage and without residual stress can be constructed. Since this study focuses on identical and isotropic materials in each layer, the coupling matrix in equation (25) can be neglected. After rearranging the equations, taking partial derivatives with respect to the x and y axes for both fields yields the shear stress field, as shown in equation (9). Using these relationships, the governing equations for the laminated plate with internal damage in the middle layer can be obtained.

III. RESULTS AND DISCUSSION

Use the finite element analysis software ANSYS to compare with the theory of this study. Figure 1 is a schematic diagram of a simulated laminated board. Boundary conditions include a fully fixed support on one side and free boundaries on the other three sides. There are no external loads applied, and the hole edges have no residual stress. The laminated plate is modeled using the fitting constraint option in ANSYS. Each layer of the laminated plate is made of 6061 aluminum alloy

with a Poisson's ratio of 0.33, Young's modulus of 69 GPa, and density of 2713 kg/m³.

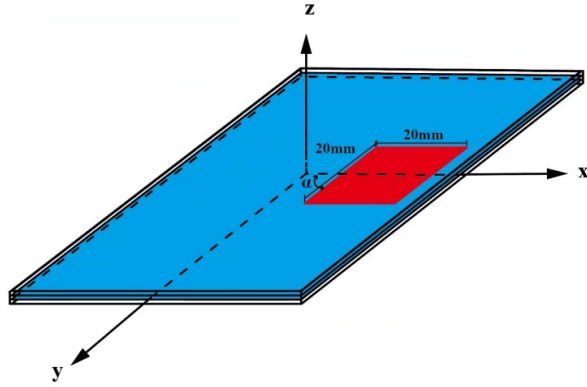


Figure 1: Schematic Diagram of the Laminated Plate

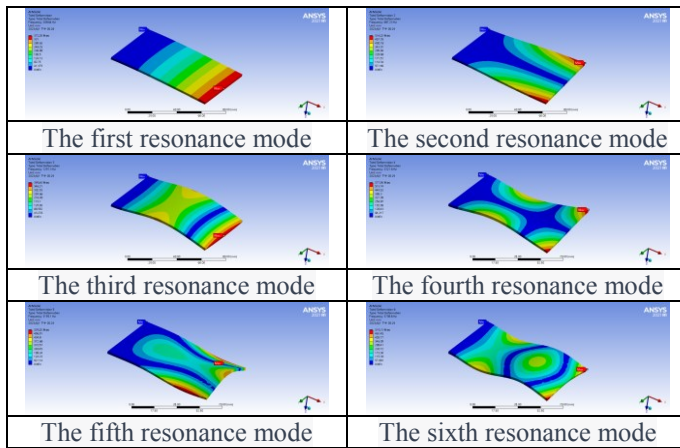


Figure 2: ANSYS simulation of undamaged laminated composite plate

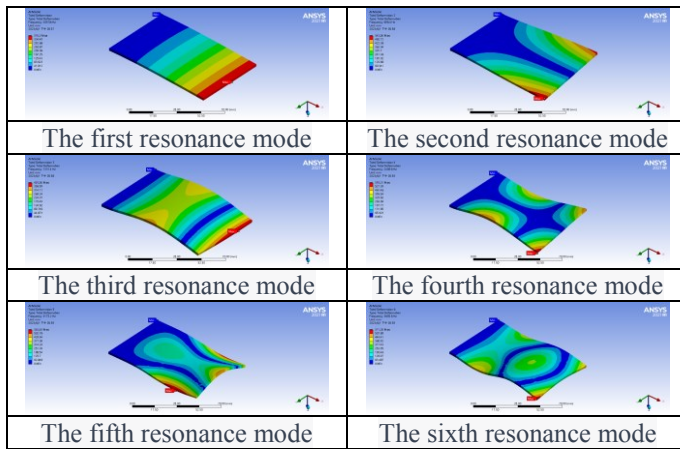


Figure 3: ANSYS simulation of damaged laminated composite plate

The upper and lower surface layers (transparent region) have dimensions of 90 mm in length, 60 mm in width, and 0.5 mm in thickness. The middle layer (blue region) has dimensions of 90 mm in length, 60 mm in width, and 1 mm in thickness. The damaged area in the middle layer (red region) has dimensions of 20 mm in length, 20 mm in width, with a y-axis

displacement of 19 mm. The angle α of the damaged region is 90°. Finite element analysis software ANSYS is utilized to analyze the difference in resonance frequencies between the undamaged laminated cantilever plate and the damaged laminated cantilever plate.

Table 1 presents the comparison of the presence or absence of damage in the laminated plate has an impact on the natural frequencies, particularly at specific frequencies where the differences are more pronounced. The influence of damaged laminated plate's natural frequencies is a critical factor in structural integrity. When unexpected impacts or fatigue occur, the natural frequencies of the structure can change, approaching or coinciding with the operating frequencies, leading to resonance phenomena. Resonance can cause an increase in stress and deformation within the structure. The simulation results indicate that the presence of damage in the laminated plate has an impact on the resonant frequencies.

Table 1: Differences of resonant frequency based on Finite Element Analysis (Laminated plate; Damage Location: y-axis displacement)

undamaged specimen (Hz)	damaged specimen (Hz)	errors (%)
208.64	209.56	-0.4
687.23	696.40	-1.3
1291.30	1331.40	-3.1
2321.60	2408.60	-3.7
3195.10	3175.20	0.6
3708.60	3605.60	2.8

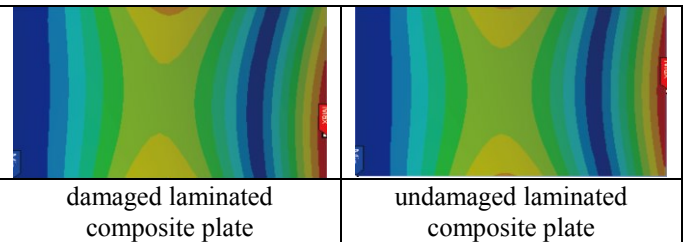


Figure 4: Comparison of the third mode
Comparing the displacements in the damaged and undamaged regions, it can be observed from Figure 4 that the displacement at the edges of the damaged area is greater than that in the undamaged laminated plate.

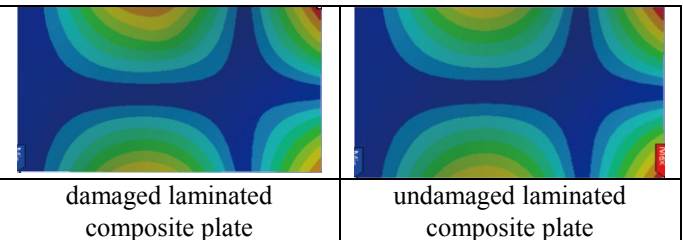


Figure 5: Comparison of the fourth mode
By comparing the displacements in the damaged and undamaged regions, it can be observed from Figure 5 that the displacement at the edges of the damaged region is greater than that in the undamaged laminated plate.

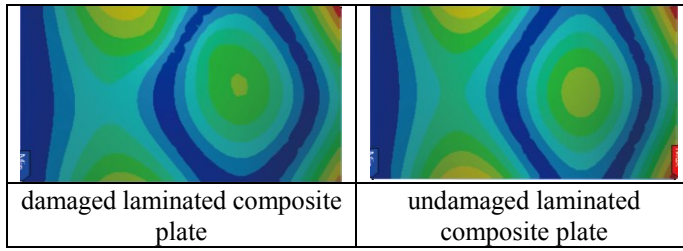


Figure 6: Comparison of the sixth mode

From Figure 6, it can be observed that the differences in nodal lines are more pronounced near the characteristic region.

From Table 1, it can be observed that the differences in resonant frequencies are more significant for the third, fourth, and fifth modes. Figures 4 and 5 show that the amplitudes near the y-axis boundary are larger in the undamaged laminated plate. Figure 6 reveals an asymmetry in the resonant modes. The internal defects accelerate damage propagation and ultimately jeopardize its safety. However, the effects of internal damage on natural frequencies in laminated plates are not always apparent and easy to predict.

Table 2: Differences of resonant frequency based on Finite Element Analysis (Single layer; Damage Location: y-axis displacement)

undamaged specimen (Hz)	damaged specimen (Hz)	errors (%)
105.04	100.36	4.5
349.11	329.06	5.8
653.45	628.78	3.8
1186.40	1219.20	-2.8
1619.30	1544.10	4.6
1893.10	1747.10	7.7

When the laminated plate is observed separately, a more pronounced difference in resonance frequency and mode shapes can be observed between the damaged and undamaged plate compared to the laminated structure as a whole. The difference in resonance frequency originates from equations (27) and (28), where the overall energy difference is due to the expansion of total kinetic energy and total strain energy with decreasing volume. Therefore, it can be inferred that the resonance frequency of a single-layer plate is inversely proportional to the extent of damage, meaning that a greater degree of damage results in a lower resonance frequency. This inference is further supported by the observed resonance frequency differences between the undamaged and damaged plate in Table 2.

IV. CONCLUSION

The location and shape of the damage can result in different influences on the natural frequencies. In real engineering applications, there are various methods of fixing the layers, and different boundary conditions at layer interfaces pose a challenging problem. The method proposed in this study can only calculate for continuous materials, treating the laminated structure as a whole. In the future, further investigation will be conducted to explore different lamination methods and

develop an approach to calculate the influence of resonance frequencies for different lamination configurations.

V. ACKNOWLEDGMENT

The authors acknowledge the financial support of this re-search by the Ministry of Science and Technology (Republic of China) under Grant MOST 112-2218-E-011-009

REFERENCES

- [1] Pei Chi Chou, Nicholas J. Pagano, *Elasticity Tensor, Dyadic, and Engineering Approaches*, Courier; 2013
- [2] C.M. Wang and J.N. Reddy and K.H. Lee, *Shear deformable beams and plates*, Elsevier Inc; 2000
- [3] Martin Sadd, *Elasticity*, Elsevier Inc; 2009
- [4] Mohamad Subhi Qatu, *Vibration of Laminated Shells and Plates*, Academic Press; 2004
- [5] Nwoji, C. U., Onah, H. N., Mama, B. O., Ike, C. C., Abd El Hady, M. E., Youssef, A. M., ... & Ren, G. (2018). *Ritz variational method for bending of rectangular Kirchhoff plate under transverse hydrostatic load distribution. Mathematical Modelling of Engineering Problems*, 5(1), 1-10.